

## Mechanical Properties of Bulk Amorphous $Ti_{50}Cu_{20}Ni_{20}Al_{10}$ Fabricated by High-energy Ball Milling and Spark-plasma Sintering

H. V. Nguyen, J. C. Kim\*, J. S. Kim, Y. J. Kwon and Y. S. Kwon

*Research Center for Machine Parts and Materials Processing,  
School of Materials Science and Engineering, University of Ulsan,  
Namgu Mugeo 2-Dong, San 29, Ulsan 680-749, Korea*

(Received August 17, 2009; Revised September 10, 2009; Accepted September 23, 2009)

**Abstract**  $Ti_{50}Cu_{20}Ni_{20}Al_{10}$  quaternary amorphous alloy was prepared by high-energy ball milling process. A complete amorphization was confirmed for the composition of  $Ti_{50}Cu_{20}Ni_{20}Al_{10}$  after milling for 30hrs. Differential scanning calorimetry showed a large super-cooled liquid region ( $\Delta T_x = T_x - T_g$ ,  $T_g$  and  $T_x$ : glass transition and crystallization onset temperatures, respectively) of 80 K. Prepared amorphous powders of  $Ti_{50}Cu_{20}Ni_{20}Al_{10}$  were consolidated by spark-plasma sintering. Densification behavior and microstructure changes were investigated. Samples sintered at higher temperature of 713 K had a nearly full density. With increasing the sintering temperature, the compressive strength increased to fracture strength of 756 MPa in the case of sintering at 733 K, which showed a 'transparent' fracture. The samples sintered at above 693 K showed the elongation maximum above 2%.

**Keywords** : Mechanical alloying, Bulk metallic glasses, Spark-plasma sintering

### 1. Introduction

Ti-based bulk metallic glasses (BMG) are regarded as highly promising materials for expanding the possible applications of bulk amorphous materials due to their light-weight, outstanding mechanical properties, and excellent corrosion resistance [1]. Amorphization of alloys is expected to bring a remarkable increase in mechanical strength and corrosion resistance. It has been reported that amorphous materials containing Ti as the main constituent element could be produced by melt spinning [2-5] in various systems such as Ti-Ni-Cu, Ti-Nb-Si-B, Ti-Ni-Cu-Al, Ti-Zr-Ni-Cu-Al and Cu-Ti-Zr-Al. However, it is fairly not easy to prepare the Ti-Cu-based BMGs with a large size. The maximum size of samples which can be produced by rapid quenching techniques is only of the order of several millimeters for as-cast Ti-based systems [6]. To overcome such limitations of the size and shape of BMGs, there have been some

attempts to produce bulk amorphous alloys by powder metallurgy processing. Mechanical alloying (MA) has proven to be an effective and relatively simple method for producing amorphous powder materials [7, 8-10]. The as-milled powder alloys are suitable for further processing; for example, bulk amorphous  $Ti_{50}Cu_{25}Ni_{20}Sn_5$  [11] and Al-La-Ni-Fe [12] alloys were consolidated by spark-plasma sintering of mechanically alloyed  $Ti_{50}Cu_{25}Ni_{20}Sn_5$  and  $Al_{82}La_{10}Ni_4Fe_4$  powders, respectively.

This work is focused on the mechanically alloyed  $Ti_{50}Cu_{20}Ni_{20}Al_{10}$  powder. The amorphous powder alloys were synthesized by high-energy ball milling [13]. Phase transformation, thermal stability and crystallization behavior of the mechanically alloyed amorphous powders were investigated. Mechanically alloyed  $Ti_{50}Cu_{20}Ni_{20}Al_{10}$  amorphous powder was consolidated by spark-plasma sintering; their microstructures and mechanical properties were investigated.

\*Corresponding Author : [Tel : +82-52-259-2231; E-mail : jckimpml@ulsan.ac.kr]

## 2. Experimental

The elemental powders of Ti, Cu, Ni, and Al with purity higher than 99% were mixed to have the final composition of  $\text{Ti}_{50}\text{Cu}_{20}\text{Ni}_{20}\text{Al}_{10}$ . MA was performed using an AGO-2 planetary ball mill with a speed of 300 rpm. Hardened steel vials and balls were used, and the ball-to-powder weight ratio was 20:1. The vials were evacuated and filled with  $5 \times 10^3$  Pa Ar gas to avoid oxidation of the powder particles. During milling, the vials were cooled by water in order to prevent an increase in temperature. The MA process was carried out using selected time-durations from 1 to 30 hrs. Each MA process was performed without interruptions. X-ray diffraction (XRD) using  $\text{Cu-K}\alpha$  radiation was used for analysis of the phase formation in the milled powder and bulk samples. Morphology of the bulk samples was observed by field emission scanning electron microscope. Powder consolidation by spark-plasma sintering was carried out in the range of super-cooled liquid region (SLR) and an applied pressure of 500 MPa, using a mold and punches made of tungsten carbide. Mechanical properties of the bulk amorphous samples were measured by micro-Vickers hardness test and compression test. Uniaxial compression test was performed to determine compressive strength for bulk amorphous samples. The sintered samples were cut by spark erosion to be cylindrical shape (3 mm in length and 2 mm in diameter). All of the compression tests were conducted using constant strain rate at  $10^{-4}$ /sec.

## 3. Results and Discussion

The progress of amorphization during milling process was monitored by means of X-ray diffraction. The XRD peaks of  $\text{Ti}_{50}\text{Cu}_{20}\text{Ni}_{20}\text{Al}_{10}$  powders with milling times ranging from 1 to 30 hrs are shown in Fig. 1. Broad halo patterns which are typical in amorphous structure can be observed after milling for 30 hrs. No diffraction peak of any crystalline

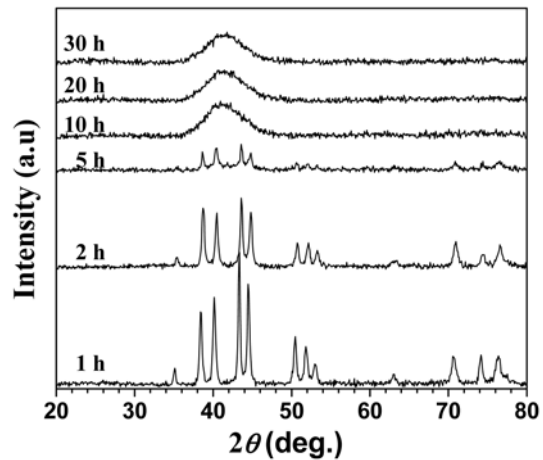


Fig. 1. XRD patterns of  $\text{Ti}_{50}\text{Cu}_{20}\text{Ni}_{20}\text{Al}_{10}$  powder as function of milling time.

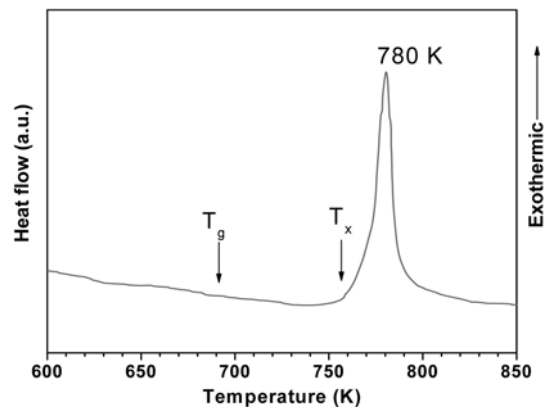


Fig. 2. DSC scans of the  $\text{Ti}_{50}\text{Cu}_{20}\text{Ni}_{20}\text{Al}_{10}$  amorphous powder, mechanically alloyed for 30 hrs.

metallic phases or oxides is indexed and a fully amorphous structure is formed.

The DSC curve of amorphous powder sample obtained from isochronous annealing at a heating rate of 10 K/min, is shown in Fig. 2. It shows that glass transition and crystallization occur at  $T_g=691$  K and  $T_x=771$  K, respectively. The alloy exhibited large super-cooled liquid region (SLR),  $\Delta T_x = T_x - T_g$ , of 80 K. It means that the produced amorphous powder is beneficial for consolidation of bulk amorphous materials.

Fig. 3(a-f) shows XRD pattern of the  $\text{Ti}_{50}\text{Cu}_{20}\text{Ni}_{20}\text{Al}_{10}$  mechanically alloyed powder compact sintered at

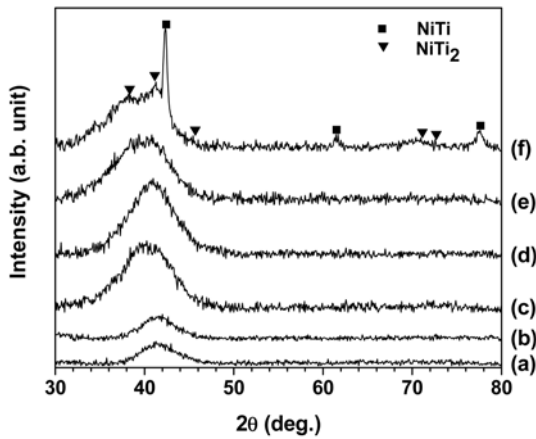


Fig. 3. XRD patterns of  $Ti_{50}Cu_{20}Ni_{20}Al_{10}$  (a) amorphous powder and bulk samples sintered at (a) 633 K, (b) 643 K, (c) 663 K, (d) 673 K, (e) 693 K and (f) 733 K, 500 MPa, 3 min holding.

various sintering temperatures in the range of 633 K and 733 K. All diffraction patterns of samples sintered below 693 K mainly consist of a broad peak and no appreciable diffraction peak corresponding to crystalline phases is detected, indicating a fully amorphous single phase in the present alloys. Sample sintered at temperature of 733 K is partially crystallized. The XRD pattern of the sintered sample still shows a halo peak with a few crystalline peaks superposed to it. The crystalline peaks are assigned to the NiTi and NiTi<sub>2</sub> intermetallic phases.

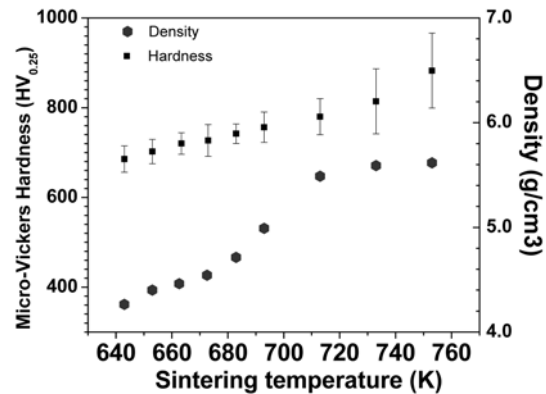


Fig. 5. Density and micro-hardness of  $Ti_{50}Cu_{20}Ni_{20}Al_{10}$  compact samples at various sintering temperatures.

Cross-section micrographs of  $Ti_{50}Cu_{20}Ni_{20}Al_{10}$  powder compact sintered at 693 K and 733 K under pressure of 500 MPa for 3 min holding time were observed with use of FE-SEM in back-scattered electron (BSE) mode and shown in Fig. 4. Higher relative density could be obtained at higher sintering temperature. Fully amorphous structure could be retained after sintering the amorphous  $Ti_{50}Cu_{20}Ni_{20}Al_{10}$  alloy at 693 K for 3 min holding time. The relative density was reached a value of 98% at sintering temperature of 733 K.

Fig. 5 shows the density and micro-hardness (Vickers scale) of amorphous  $Ti_{50}Cu_{20}Ni_{20}Al_{10}$  alloy powder compact sintered at different temperature. It can be

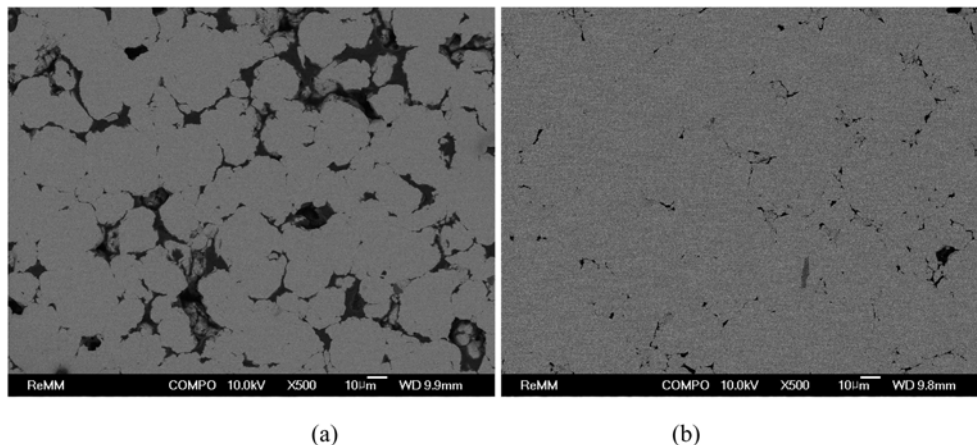


Fig. 4. BSE micrographs of the cross-section of  $Ti_{50}Cu_{20}Ni_{20}Al_{10}$  bulk samples sintered at (a) 693 K and (b) 733 K.

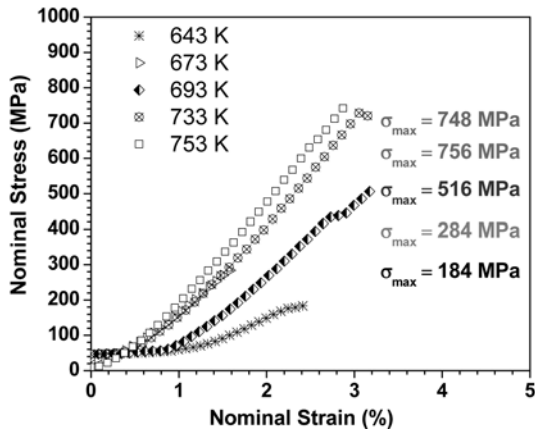


Fig. 6. Compression test of sintered samples at various temperatures.

seen that the density increased only gradually from 663 K to 673 K, whereas it increased rapidly from 673 K to 713 K. The samples sintered at the temper-

ature above 713 K had a nearly full density. Hardness value increased with the increasing sintering temperature. The high hardness value of 814 and 883  $HV_{0.25}$  can be obtained at sintering temperature of 733 K and 753 K, respectively.

The stress-strain curves obtained from the compression tests are given in Fig. 6 for various sintering temperatures. The compacts sintered at temperature of 643 K and 673K show low compressive strength which is most likely due to the residual porosity (Fig. 7(a) and (b)). The highest compressive strength of 756 MPa was obtained for samples sintered at temperature higher than 733 K. Further increasing of sintering temperature led to decrease in compressive strength, which was due to a higher portion of inter-metallic phases.

SEM images of fracture surface of the compression-test specimen sintered at 673 K, 693 K, 733

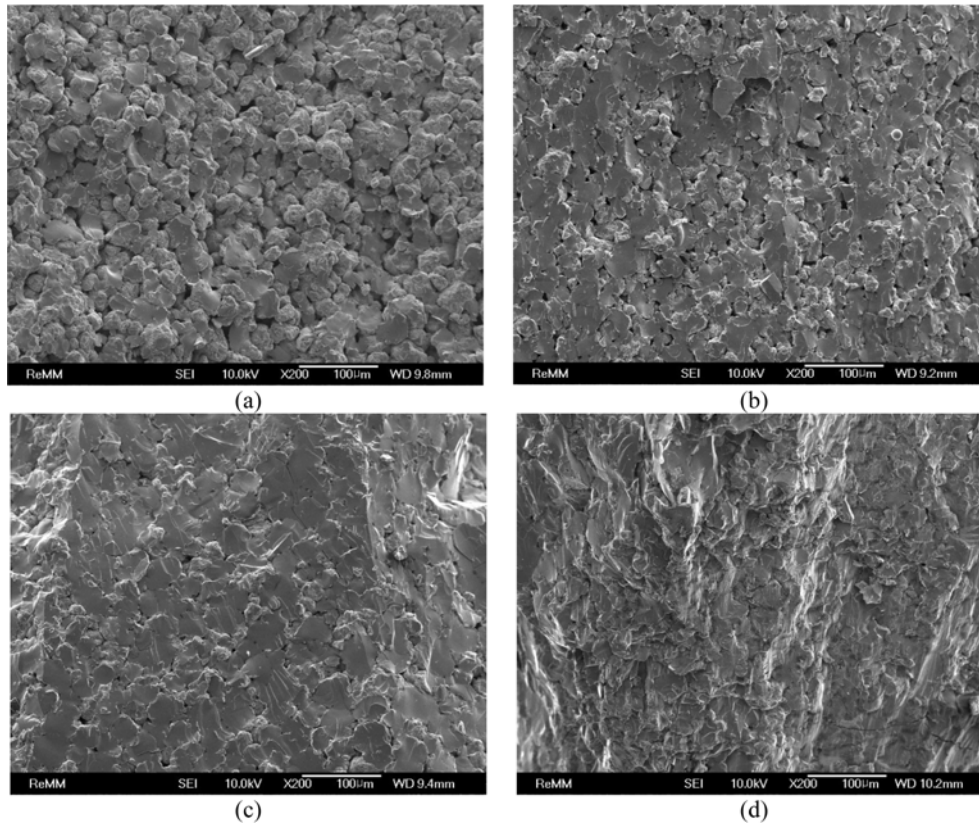


Fig. 7. Fracture surface of post-compressive test of samples sintered at (a) 673 K, (b) 693 K, (c) 733 K and (d) 753 K.

K and 753 K are given in Fig. 7. It can be seen that interparticle boundaries may still exist and the bonding between the powder particles may not be sufficient to reach higher strength value of the fracture (Fig. 7a). Sample sintered at 673 K, Fig. 7(b), shows relatively high density of voids. At higher sintering temperatures of 693 K and 733 K, the voids were removed rapidly. A higher portion of 'transparent' rupture was observed at higher sintering temperatures. But the void still exist and it shows a low portion of interparticle boundaries, as seen in Fig. 7(c), which may result in the low compressive strength as discussed above. The results indicate that external applied pressure was not sufficient for consolidation even though sintering temperature was as high as 733 K. The compressive stress-strain behavior of the  $Ti_{50}Cu_{20}Ni_{20}Al_{10}$  compact sample sintered at 693 K, 733 K and 753 K exhibited elongation maximum above 2%.

#### 4. Conclusions

Bulk-metallic glass powder compacts were successfully fabricated using a combination of mechanical alloying and SPS processes. Sintering at higher than 733 K led to a partial crystallization and peaks of NiTi and NiTi<sub>2</sub> intermetallic phases could be detected in XRD pattern. The samples sintered at temperature above 713K had a nearly full density. With increasing sintering temperature, the compressive strength increased to fracture strength of 756 MPa in the case of sintering at 733 K, which showed

a 'transparent' fracture. The compressive stress-strain curve of the samples sintered at above 693K showed elongation maximum above 2 %.

#### Acknowledgments

This work was financially supported by the Korea Governments (MOEHARD)(KRF-2006-2110D00221).

#### References

- [1] Y. C. Kim, W. T. Kim and D. H. Kim: Mater. Sci. Eng. A., **375** (2004) 127.
- [2] T. Zhang and A. Inoue: Mater. Trans. JIM., **39** (1998) 1001.
- [3] A. Inoue, N. Nishiyama, K. Amiyama, T. Zhang and T. Masumoto: Mater. Lett., **19** (1994) 131.
- [4] K. Amiya, N. Nishiyama, A. Inoue and T. Masumoto: Mater. Sci. Eng. A., **179** (1994) 692.
- [5] A. Inoue: Mater. Sci. Forum., **312** (1999) 307.
- [6] D. V. Louzguine and A. Inoue: Scripta. Mater., **43** (2000) 371.
- [7] A. W. Weeber and H. Bakker: Physica B: Condensed Matter., **153** (1988) 93.
- [8] C. C. Koch, O. B. Cavin, C. G. McKamey and J. O. Scarbrough: Appl. Phys. Lett., **43** (1983) 1017.
- [9] M. S. El-Eskandarany, K. Aoki and K. Suzuki: J. Less-Common Met., **167** (1990) 113.
- [10] T. S. Kim, J. K. Kim, H. J. Kim and J. C. Bae: Mater. Sci. Eng. A., **402** (2005) 228.
- [11] P. P. Choi, J. S. Kim, O. T. H. Nguyen and Y. S. Kwon: Mater Lett., **61** (2007) 4591.
- [12] P. P. Choi, J. S. Kim, O. T. H. Nguyen, D. H. Kwon, Y. S. Kwon and J. C. Kim: Materials Science and Engineering A, **449** (2007) 1119.
- [13] N. H. Viet, J. C. Kim, J. S. Kim and Y. S. Kim: J. Korean Powder Metall. Inst., **16** (2009) 9 (Korean).